Journal of Electron Devices, Vol. 17, 2013, pp. 1476-1485

© JED [ISSN: 1682 -3427]

Journal of Electron Devices
www.jeldev.org

THE ELECTRICAL PROPERTIES OF InGaN/GaN/AlN MSM PHOTODETECTOR WITH Au CONTACT ELECTRODES

Zehor Allam[1], Abdelkader Hamdoune, Chahrazed Boudaoud

Unity of Research "Materials and Renewable Energies", Faculty of Sciences, University of Abou-bekr Belkaid, PO Box 230, 13000, Tlemcen, ALGERIA
[1] zh1344@yahoo.fr

Received 25-03-2013, online 02-04-2013

ABSTRACT
In this paper, we consider an InGaN/GaN/AlN ultraviolet (UV) photodetector. We first describe internal characteristics.The device exhibited a very good current of about 1.25mA.The variation of photocurrent versus optical wavelength demonstrates a peak of 0.6 µA at a wavelength of 402 nm, under -0.5 V bias.
Keywords: Gallium nitride (GaN), aluminum nitride (AlN), aluminum gallium nitride (InGaN), UV photodetector.

I. INTRODUCTION

Detection of ultraviolet (UV) has become increasingly important in a number of areas, such as flame detection, water purification, astronomy , UV ultraviolet radiation dosimetry, lithography aligners, combustion control systems, solar UV monitoring, space-to-space communications, detection of missiles etc. [1]. Recently, Nitride-based semiconductors have attracted much attention as promising materials for light emitting diodes, laser diodes.... These materials are also capable of detecting ultraviolet light. The main reason is that nitride based materials have wide band gaps, high drain current density, high saturation velocity and high breakdown field [2]. It is known that UV radiation is safe for the human body. More exposed to UV rays can cause diseases such as skin cancer. Thus, the detection of UV light has become an important issue [3].

In the past few years, MSM photodiodes have become increasingly popular in the research field due to their fundamental advantages [4,5]:

- Simple structure.
- Ease of fabrication and integration.
- Low capacitance per unit area.

MSM photodiodes are comprised of two back-to-back Schottky diodes by using an interdigitated electrode configuration on top of an active light collection region.

This photodetector cannot operate at a zero bias. MSM photodiodes are inherently fast due to their low capacitance per unit area and are usually transit time limited, not time constant limited. With electron beam lithography, the electrode width and spacing can be made with submicron dimension which greatly improves the speed. The biggest drawback of MSM photodetectors is their intrinsic low responsivity. MSM detectors exhibit low photoresponsivity mainly because the metallization for the electrodes shadows the active light collecting region.

In new technologies, the need for high quality materials AlN, GaN, InN and their alloys AlGaN, InGaN is a condition essentially. The basic research is very important to understand the mechanisms of growth and thus improve the quality of materials controlling the growth conditions and also exploring new ways to implement the ability of modern growth [6].

II. SIMULATION AND MODELING

"Atlas" is a simulator 3D and 2D device based on semiconductor physics. He predicts the electrical behavior of semiconductor structures specified and provides insights into the physical mechanisms associated with the internal operation of the devices. Atlas can be used independently or as a tool in the kernel environment simulation VWF (Virtual Wafer Fab) of SILVACO. In order to predict the impact of process variables on the behavior of circuit simulation device attached simulation of the process model and the extraction of SPICE (Simulation Program with Integrated Circuit Emphasis) [7].

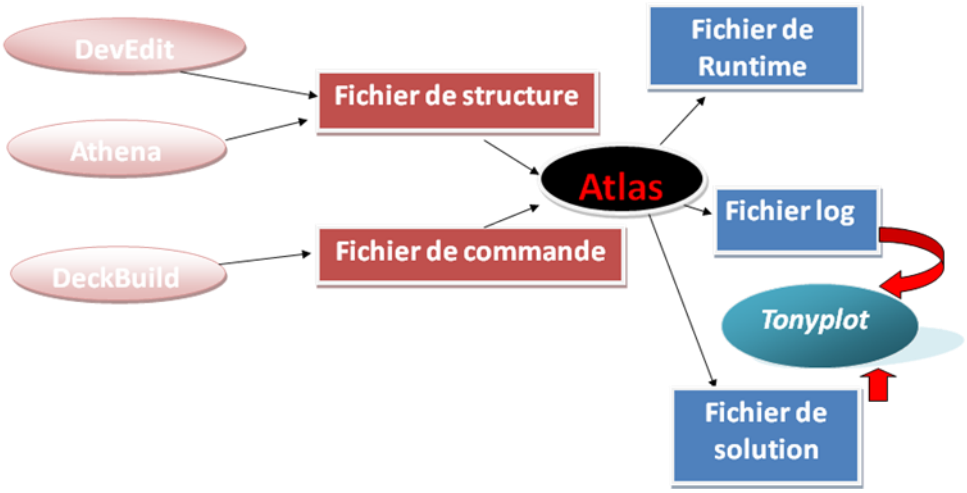

Fig.1: Inputs and outputs of Atlas.

The proposed structure of InGaN/GaN/AlN UV photodetector is shown in Fig.2; it was simulated using ATHENA and ATLAS in SILVACO TCAD device simulation.However, thin GaN window layers, designed in a 2 – 10 nm thickness range, are typically strained due to lattice mismatch with the underlying InGaN layer and hence, generate substantial piezoelectric polarization.

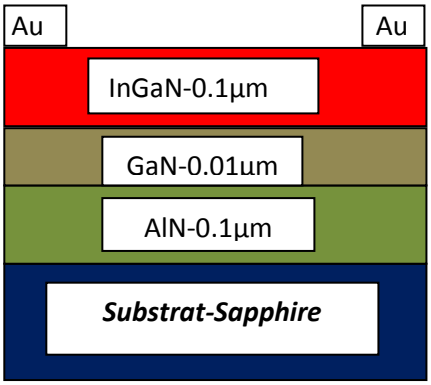

Fig.2: Structure of studied MSM UV photodetector with gold electrodes.

The detector is based on a 0.1µm thick InGaN epitaxial layers grown on sapphire substrate by metalorganic chemical vapor deposition (MOCVD)[8]. The sample InGaN / GaN / AlN consisted of a temperature of 0.01 µm thick low (550-C) GaN layer, at 0.1 µm of InGaN thick at high temperature (1050-C) N layer unintentionally doped, a layer 0.1µm thick temperature (1100-C) undoped AlN interlayer and 0.3µm thick Sapphire. With 250 nm of Au film was then deposited on the sample by RF magnetron sputtering.

The energy band diagram has been simulated using BLAZE tool, which is interfaced with ATLAS is a general purpose 2-D device simulator for III–V, II–VI materials, and devices with position dependent band structure (i.e., heterojunctions) [6]. BLAZE accounts for the effects of positionally dependent band structure by modifications to the charge transport equations.

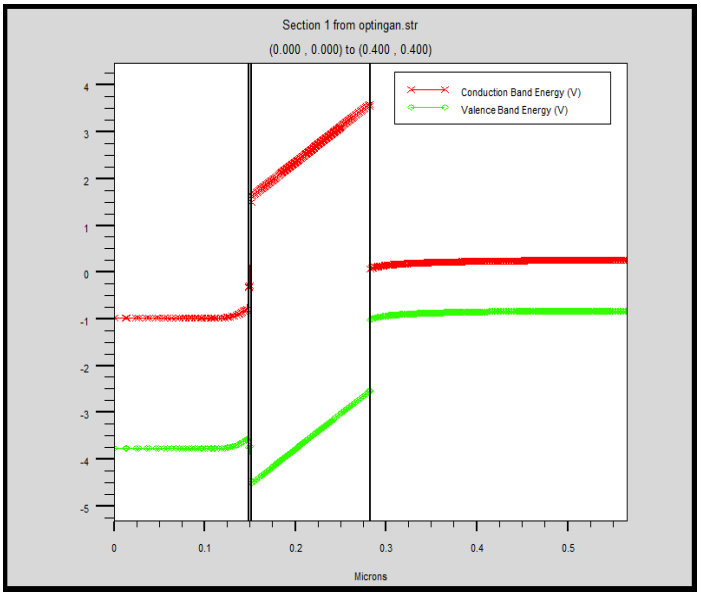

Fig.3: Energy band diagram.

The numerical simulation of MSM photodetector has been carried out for non-degenerate semiconductor and parabolic shape of conduction band. The simulation involves solution of five decoupled equations using Newton's iteration technique.

The Fermi–Dirac statistic for parabolic shape of conduction band has been taken in all the calculations of carrier and doping densities.

For the simulation of I-V current associated with MSM photodetector; radiative recombination (R_c), recombination rate (R_{SRH}), Auger recombination (R_{Auger}), and surface recombination (R_{surf}) rates, are modeled as:

$$R_c^{opt} = C_c^{opt}(pn - n_i^2) \quad (1)$$

$$R_{SRH} = \frac{pn - n_i^2}{\tau_{pO}\left[n + n_i \times \exp\left(\frac{E_t}{kT}\right)\right] + \tau_{nO}\left[p + n_i \times \exp\left(-\frac{E_t}{kT}\right)\right]} \quad (2)$$

$$R_{Auger} = C_n(pn^2 - nn_i^2) + C_p(p^2 n - pn_i^2) \quad (3)$$

$$R_{surf} = \frac{pn - n_i^2}{\tau_p^{eff}\left[n + n_i \times \exp\left(\frac{E_t}{kT}\right)\right] + \tau_n^{eff}\left[p + n_i \times \exp\left(-\frac{E_t}{kT}\right)\right]} \quad (4)$$

Here C_c^{opt} is the capture rate of carriers; C_n and C_p are Auger coefficients for electrons and holes respectively; n and p are equilibrium electron and hole concentration, E_t is energy level of trap; n_i is intrinsic carrier concentration; τ_{n0} and τ_{p0} are SRH lifetime of electrons and holes respectively; τ_n^{eff} and τ_p^{eff} are effective life times of electrons and holes [9].

III. RESULTS AND DISCUSSION

ATLAS does not contain all necessary properties of InGaN/GaN/AlN-based material; the following properties were added for accurate results.
The relationship between the band gap energy (Eg) and the indium fraction (x) were proposed using Vegard's Law modified by a bowing parameter (b):

$$E_g(x) = x \times E_g(InN) + (1-x) \times E_g(GaN) - b \times (1-x) \times x \quad (5)$$

where E_g(AlN) = 6.28 eV; $Eg._{GaN}$ =3.42 eV; $Eg._{InN}$ = 0.77 eV and b =1.43 eV [10].

The electric field generated within the depletion region of the device is caused by the difference in the Fermi levels on either side of the heterojunction. High electric field exists in the GaN /AlN layer; it is found of 1.25×10^5 V / cm at room temperature. Consequently, it

prevents the appearance of the parasitic channel that would otherwise form in the undoped AlN layers [11].

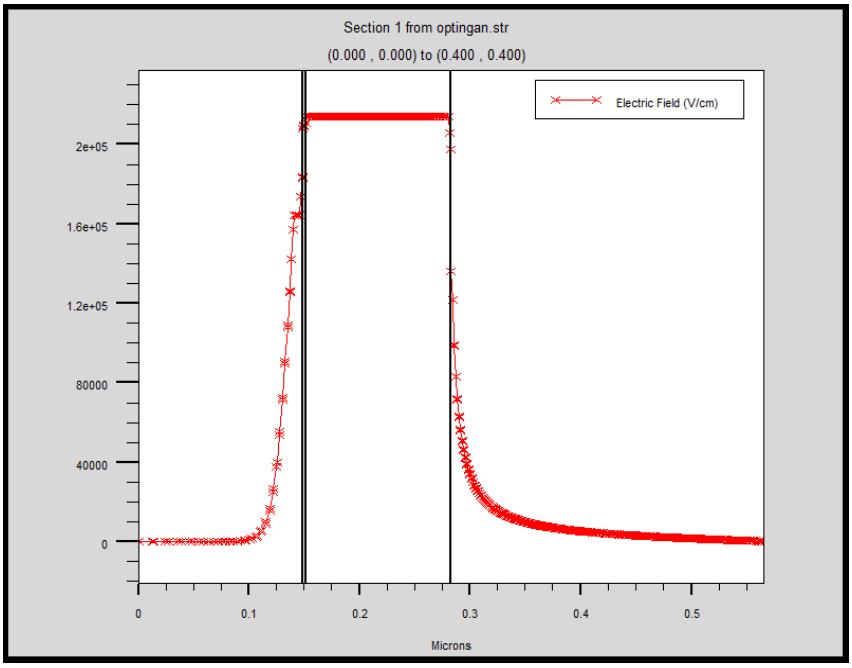

Fig.4: Simulated electric field profile in absence of external biasing.

These results include the influence of electric fields caused by the piezoelectric polarization induced by the stress in the InGaN and spontaneous polarization.

In the interface metal /semiconductor is a potential barrier for electrons is the difference in work function between the metal and the semiconductor.

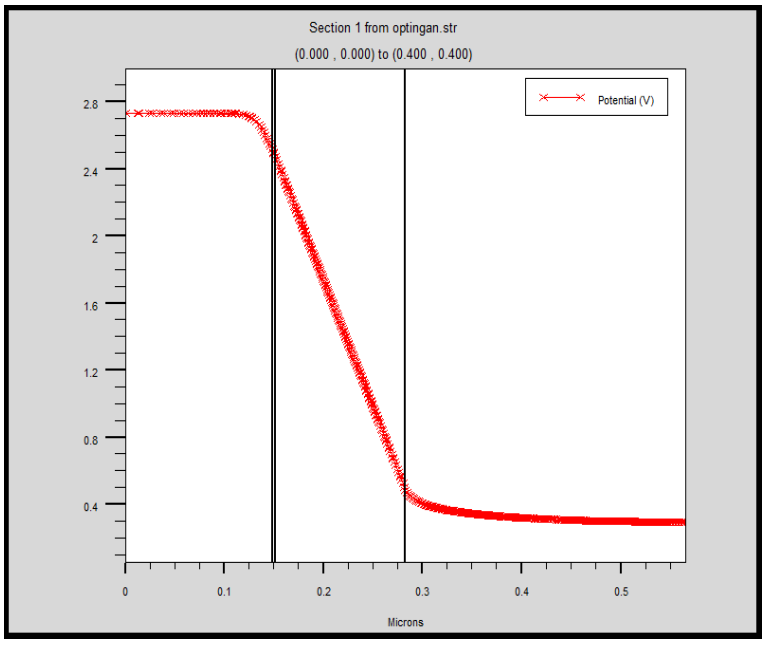

Fig.5: InGaN/GaN/AlN internal potential.

This causes the formation of heterojunction a potential well in the small-gap material in which electrons from the donor layer are transferred and accumulated. The heterojunction is characterized by the discontinuity of the energy of the conduction band between the two materials, plus the value of the energy of the conduction band is high, the electron transfer from the donor layer to the channel will be better In addition, over the material of the channel will be small gap, the transport properties (speed, mobility) will be better.

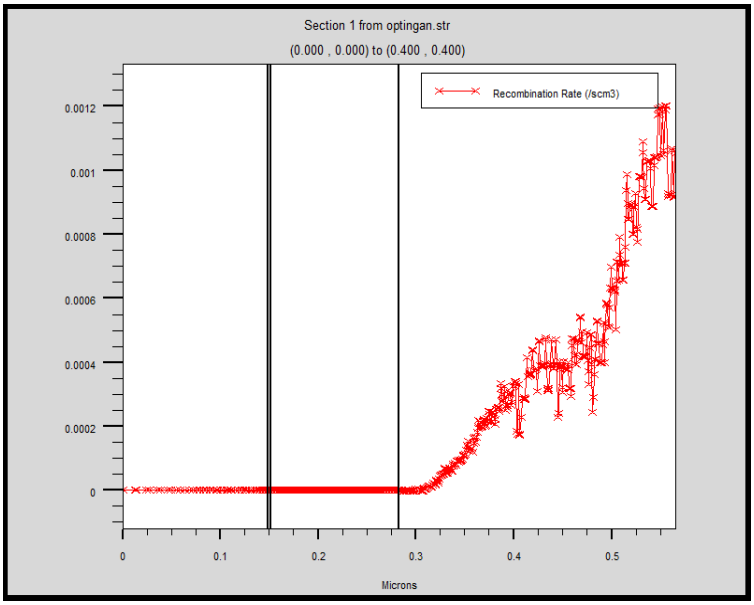

Fig.6: Recombination rate in the InGaN/GaN/AlN structure.

The simulated variation of recombination rate with layer thickness of the device in illuminated is shown in Fig.6. Generation recombination (GR) component of current is due to defects within the depletion region which acts as intermediate states for the thermal generation and recombination of carriers.

These intermediate states are referred to as Schockley Read centers. The generation recombination component of current density can be approximated as in references [12, 13].

Defect related recombination is known to be the main carrier loss mechanism in nitride devices. The Shockley– Read–Hall (SRH) recombination lifetime of electrons and holes is assumed to be 1 ns [14].

The simulated current density is shown in Fig.7. We observe a high value of current density in the layer InGaN : 0.023 A/cm^2 for reverse bias up to 0.2 V.

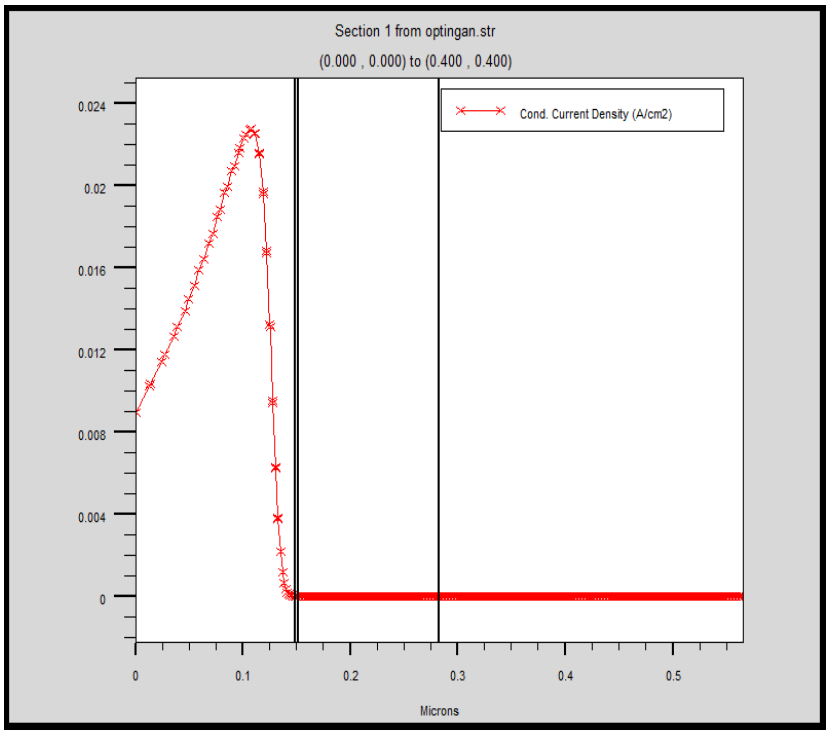

Fig.7: Conduction current density.

The current density increases because it absorbs a larger fraction of the photons with energies larger than 2.1 eV. Therefore, one must decrease the bandgap of the InGaN junction so that it also absorbs more photons.

The mechanism of optical gain in InGaN quantum wells of UV photodetector real is not yet fully understood. It can be strongly affected by non-uniform distribution. Internal bias fields tend to separate quantum confined electrons and holes, which reduces the optical gain and spontaneous emission. However, the screening of the electrons and holes are provided to remove bias fields at high current operation [15].

A Schottkey Contact is formed between the InGaN and Au metal determined by the I-V curve measured between Au and InGaN. Also it is confirmed by Electron Beam induced current measurements. The diode has an apparently rectifying current characteristic.

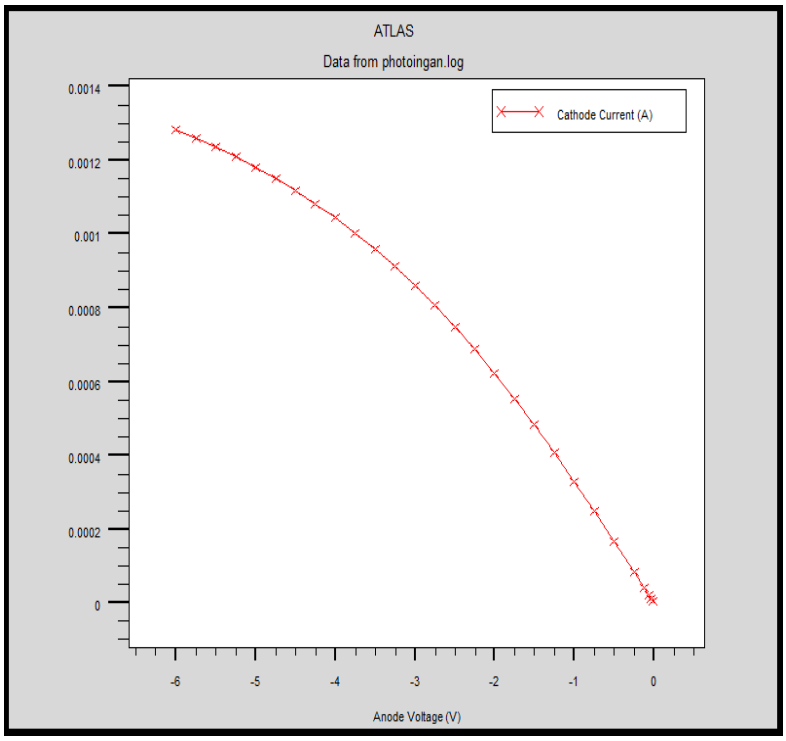

Fig.8: I-V curve in InGaN/GaN/AlN photodetector.

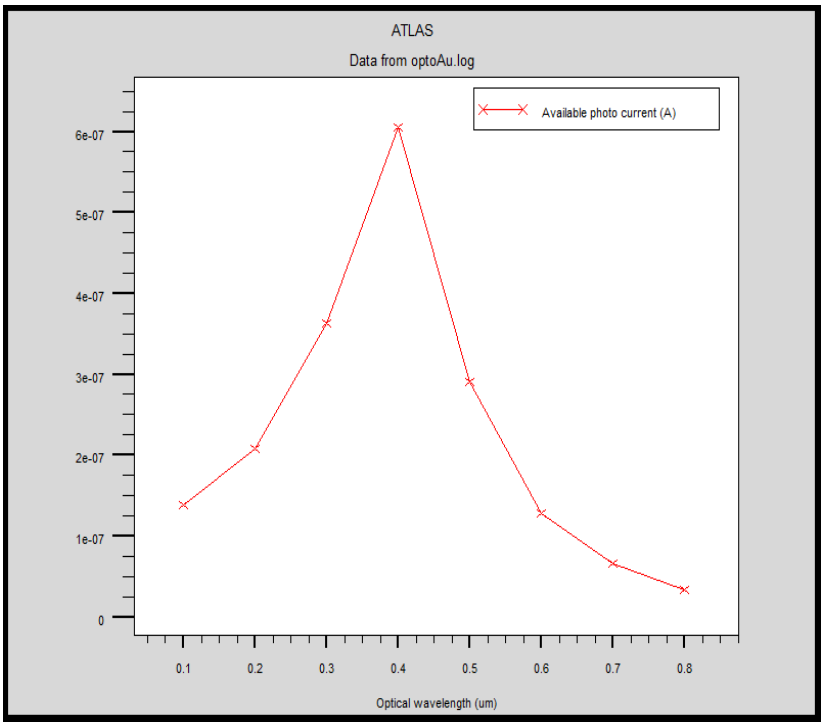

Fig.9: Photocurrent as a function of optical wavelength, for -0.5V.

Fig.8 shows I–V characteristics of the simulated InGaN/GaN photodetector.

We find a current of about 1.25 mA it was found for -6V applied bias this is in good agreement with the experimental value of current.

The variation of photocurrent of InGaN/GaN/AlN photodetector as a function of wavelength at a bias voltage of -0.5V is shown in Fig.9. We can optimize the performance of the device by changing the doping concentration and dimensions of the device for high bandwidth performance. The device exhibits at a wavelength of 402 nm, a responsivity peak of 0.6µA.

IV. CONCLUSION

In this paper, we studied an InGaN/GaN/AlN photodetector device. Modeling and simulation were performed by using ATLAS-TCAD simulator. Energy band diagram, conduction current density, Recombination rate, internal potential and electric field were performed.

The device exhibited a very good current of about 1.25mA.The variation of photocurrent versus optical wavelength demonstrates a peak of 0.6 µA at a wavelength of 402 nm, under -0.5 V bias.

The simulation and modeling described in this work can be used for optimizing the existing ultraviolet detectors and developing new devices.

References

[1] Nidhal. N. Jandow, Kamarul Azizi Ibrahim , Haslan Abu Hassan, Sabah M. Thahab, and Osama S Hamad, "The electrical properties of ZnO MSM Photodetector with Pt Contact Electrodes on PPC Plastic" Journal of Electron Devices, **7**, 225-229 (2010).

[2] H. Mosbahia, M. Gassoumia, H. Mejrib, M. A. Zaidia, C. Gaquierec, H. Maarefa. "Electrical Characterization Of AlGaN/GaN HEMTs ON Si Substrate" Journal Of Electron Devices, **15**, 1225-1231 (2012).

[3] Sheng-Po Chang, Shoou-Jinn Chang, Chien-Yuan Lu, Yu-Zung Chiou, Ricky W. Chuang, and Hung-Chieh Lin, "Low-frequency noise characteristics of GaN-based UV photodiodes with AlN/GaN buffer layers prepared on Si substrates" J. Crystal Growth **311**, 3003-3006 (2009).

[4] Gao W.; Khan A.; Berger P.R.; Hunsperger R.G.; Zydzik G.; O'Bryan H.M.; Sivco D.; Cho A.Y., "$In_{0.53}Ga_{0.47}As$ Metal-Semiconductor-Metal Photodiodes with Ransparent Cadmium Tin Oxide Schottky Contacts" Appl. Phys. Letts. **65**, 1930-1932 (1994).

[5] Su Y.K.; Chiou Y.Z.; Juang F.S.; Chang S.J.; Sheu J.K. " GaN and InGaN Metal-Semiconductor-Metal Photodetectors with Different Schottky Contact Metals" Jpn. J. Appl. Phys. **40**, 2996-2999 (2001).

[6] Pierre Masri, "Silicon carbide and silicon carbide-based structures, the physics of epitaxy", Surface Science Reports **48**, 1-51 (2002).

[7] ATLAS User's Manual Version 5.10.0.R, SILVACO International, Santa Clara, CA 95054, 2005.

[8] Guozhen SHEN, Di CHEN, "One-dimensional nanostructures for electronic and optoelectronic devices", Front. Optoelectron. China **3**, 125–138 (2010).

[9] A.D.D. Dwivedi, A. Mittal, A. Agrawal, and P. Chakrabarti, "Analytical modeling and ATLAS simulation of N^+-InP/n0-$In_{0.53}Ga_{0.47}As$/p^+-$In_{0.53}Ga_{0.47}As$ p-i-n photodetector for optical fiber communication", Infrared Physics & Technology **53**, 236–245 (2010).

[10] J. Wu, W. Walukiewicz, K.M. Yu, J.W. Ager III, E.E. Haller, H. Lu, W.J. Schaff, "Small band gap bowing in $In_{1-x}Ga_x/N$ alloys," Appl. Phys. Lett. **80,** 4741-4743 (2002).

[11] Hadis Morkoc, Aldo Di Carlo, and Roberto Cingolani, "GaN-based modulation doped FETs and UV detectors", Solid-State Electronics **46**, 157–202 (2002).

[12] V. Gopal, S.K. Singh, R.M. Mehra, "Analysis of dark current contributions in mercury cadmium telluride junction diodes", Infrared Physics and Technology **43**, 317-326 (2002).

[13].P. Chakrabarti, A. Krier, A.F. Morgan, "Analysis and simulation of a mid-infrared $P+InAs_{0.55}Sb_{0.15}P_{0.30}/n0-InAs_{0.55}Sb_{0.11}/N^{+}-InAs_{0.55}Sb_{0.15}P_{0.30}$ double heterojunction photodetector grown by LPE", IEEE Trans. on Electron Devices **50**, 2049–2058 (2003).

[14] Park S.H., Chuan S.L., "Piezoelectric effects on electrical and optical properties of wurtzite GaN=AlGaN quantum well lasers", Appl. Phys. Lett. **72**, 3103–3105 (1998).

[15] Dmitriev A.V., Oruzheinikov A.L. 'The rate of radiative recombination in the nitride semiconductors and alloys".MRS Internet J. Nitride Semicond. Res. **1**, 46 (1996).